Free Radical Biology & Medicine 47 (2009) 1494–1506

Contents lists available at ScienceDirect

Free Radical Biology & Medicine

journal homepage: www.elsevier.com/locate/freeradbiomed

Original Contribution

Role of a differentially expressed cAMP phosphodiesterase in regulating the induction of resistance against oxidative damage in *Leishmania donovani*

Arijit Bhattacharya [1], Arunima Biswas [1], Pijush K. Das *

Molecular Cell Biology Laboratory, Indian Institute of Chemical Biology, Kolkata 700032, India

ARTICLE INFO

Article history:
Received 24 April 2009
Revised 4 June 2009
Accepted 20 August 2009
Available online 3 September 2009

Keywords:
Leishmania donovani
Macrophage
Oxidative stress
cAMP phosphodiesterase
Free radicals

ABSTRACT

Differentiation-coupled induction of resistance of *Leishmania* parasites to macrophage oxidative damage was shown to be associated with an increased cAMP response. This study explores the significance of the cAMP response in the parasite by identifying a differentially expressed cAMP phosphodiesterase (LdPDEA) and deciphering its role in regulating antioxidant machineries in the parasite. LdPDEA, a high K_M class I cytosolic cAMP phosphodiesterase, was expressed maximally in log-phase promastigotes, but was significantly reduced in stationary-phase promastigotes and amastigotes. Chemical inhibition or silencing of PDEA conferred enhanced resistance to pro-oxidants in these cells and this led to studies on trypanothione biosynthesis and utilization, as trypanothione is one of the major modulators of antioxidant defense in kinetoplastidae. Despite enhanced arginase and ornithine decarboxylase activity, trypanothione biosynthesis seemed to be unaffected by PDEA blockage, whereas significant elevations in the expression of tryparedoxin peroxidase, ascorbate peroxidase, and tryparedoxin were detected, suggesting a definite shift of trypanothione-pool utilization bias toward antioxidant defense. Moreover, parasites that overexpressed PDEA showed reduced resistance to oxidative damage and reduced infectivity toward activated macrophages. This study reveals the significance of a cAMP phosphodiesterase in the infectivity of *Leishmania* parasites.

In the course of its digenetic life cycle, *Leishmania donovani,* the causative agent of a fatal visceral form of leishmaniasis, undergoes transformation from an insect-vector-borne procyclic promastigote form to an intracellular vertebrate-host-specific amastigote form. At the onset of vertebrate host entry, the parasite encounters tremendous oxidative stress due to radicals generated by oxidative bursts in the actively phagocytizing macrophages. Still, a subset of the parasite survives, proliferates intracellularly, and establishes infection. The exact molecular mechanisms by which *Leishmania* circumvents the toxic effects of pro-oxidants during macrophage invasion are not fully understood. Although the parasite possesses at least two superoxide dismutases, the kinetoplastidae are characterized by the absence of a functional catalase. Peroxide detoxification, therefore, depends entirely on thiol-based antioxidants, among which trypanothione (N^1,N^8-(bisglutathionyl) spermidine; TSH) is the most important [1]. TSH, a trypanosome-specific unique dithiol, together with trypanothione reductase, tryparedoxin, and tryparedoxin peroxidase, comprises the trypanothione peroxidase system, one of the major antioxidant machineries of the parasite [2]. TSH biosynthesis occurs through a complex biochemical cascade to yield spermidine from arginine via arginase, ornithine decarboxylase (ODC), and spermidine synthase [1,3]. The cascade depends considerably on the availability of precursors. For *Leishmania,* high-affinity arginine, as well as polyamine transporters (LdAAP3 and LmjPOT1), is active but reportedly nonessential, and there are predictively more than one of such transporters present, which differ in their biochemical properties [4,5]. TSH provides the reduction equivalents for ribonucleotide reductase, an essential enzyme for nucleotide biosynthesis, and for tryparedoxin peroxidase and ascorbate peroxidase, two major antioxidant enzymes [6]. An intermediate electron acceptor, tryparedoxin catalyzes the process of electron transfer from TSH to ribonucleotide reductase and tryparedoxin peroxidase [1]. TSH gains further importance as it forms thiol conjugates with trivalent antimony and arsenic compounds for subsequent efflux of antimonials and arsenicals leading to drug resistance in the parasite [7].

Among many environmental sensing pathways, the cAMP-mediated response plays a major role in differentiation and cellular transformation of many unicellular eukaryotes [8–10]. In *Trypanosoma brucei* cAMP-mediated events are responsible for differentiation from the bloodstream form to the stumpy form [11]. The *Leishmania* genome

Abbreviations: 8-BrcAMP, 8-bromo-cAMP; pCPTcAMP, parachlorophenylthio-cAMP; PDE, phosphodiesterase; FCS, fetal calf serum; IBMX, 3-isobutyl-1-methylxanthine, ODC, ornithine decarboxylase; ORF, open reading frame; PBS, phosphate-buffered saline; ROS, reactive oxygen species; H_2DCFDA, 2′,7′-dihydrodichlorofluorescein diacetate; LdPDEA, *L. donovani* cAMP phosphodiesterase A; MTT, 3-(4,5-dimethyldiazol-2-yl)-2,5-diphenyltetrazolium bromide; GSH, reduced glutathione; TSH, reduced trypanothione; RNI, reactive nitrogen species.

* Corresponding author. Fax: +91 33 2473 5197.
E-mail address: pijushdas@iicb.res.in (P.K. Das).

[1] These authors contributed equally to this work.

0891-5849/$ – see front matter © 2009 Elsevier Inc. All rights reserved.
doi:10.1016/j.freeradbiomed.2009.08.025

sequence suggests the presence of genes required for a definitive cAMP response in the organism and recent reports provide evidence for cAMP-regulated events in metacyclogenesis and stress response [12,13]. Intracellular cAMP levels are regulated by adenylate cyclase and phosphodiesterase (PDE). A receptor adenylate cyclase from *L. donovani* has been characterized and the mechanism of catalysis of its homologues and their importance in the differentiation-associated stress response in *Trypanosoma* have been reported [14–17]. However, despite the identification and characterization of a number of PDEs from *Trypanosoma* and *Leishmania,* no significant functional importance of PDE has been proposed to date. All the PDEs (A, B1, B2, and C) that have been identified from trypanosomes belong to the class I PDE family with an ~270-amino-acid-long phosphodiesterase catalytic domain (PDEase I). PDEB1 and B2 from *T. brucei* and *T. cruzi* are cAMP-specific, having GAF domains, and are localized in the flagellar pocket, but PDEC, although dual-specific, is localized on the vesicular membrane with an N-terminal FYVE domain [18,19]. PDEA, on the other hand, is a magnesium-dependent cytosolic enzyme [20,21]. Although the *Leishmania* genome sequence suggests the presence of homologues of all the above-mentioned PDEs, LmjPDEB1, B2, and A have recently been cloned and sequenced from *L. major* [22]. Furthermore, PDEB1 and PDEB2 have been biochemically and structurally characterized [23]. In our previous study, we showed that modulation of PDE activity induced resistance to peroxide and peroxynitrite in *L. donovani* [13]. In this study, we present evidence for LdPDEA being a differentially expressed, cAMP-specific enzyme having a high impact on peroxide metabolism through TSH. Furthermore, we demonstrate that PDEA regulates polyamine biosynthesis in the parasite and may have a role in parasite infectivity in terms of TSH pool utilization bias for antioxidant defense.

Experimental procedures

Parasite and cell culture

Pathogenic strains of *L. donovani,* AG83 (MHOM/IN/1983/AG83) and GE1 (MHOM/IN/89/GE1), were maintained in susceptible BALB/c mice and cultured as promastigotes in medium 199 (Invitrogen, Carlsbad, CA, USA) with Hanks' salt containing Hepes (12 mM), L-glutamine (20 mM), 10% heat-inactivated FCS, 50 U/ml penicillin, and 50 μg/ml streptomycin. The promastigotes were obtained by culturing infected spleens in medium M199 for 5 days at 22°C. The adherent murine macrophage cell line RAW 264.7 was cultured at 37°C with 5% CO_2 in RPMI 1640 (Invitrogen) supplemented with 10% FCS, 100 U/ml penicillin, and 100 μg/ml streptomycin.

Differentiation conditions and viability assay

For exposure to differentiation conditions, medium 199 containing promastigotes was titrated to pH 5.5 with 10 mM succinate–Tris and incubated at 37°C with 5% CO_2. Viability assay of promastigotes exposed to varying concentrations of H_2O_2 and $ONOO^-$ was carried out by incubation in 0.5 mg/ml 3-(4,5-dimethylthiazol-2-yl)-2,5-diphenyltetrazolium bromide (MTT) as described earlier [24].

Cloning and expression of L. donovani phosphodiesterase A

Sequences corresponding to the PDEA ORF were amplified using the primers 5′-GGAATTCCATATGCTCGACTTTCTTGAGCAG-3′ (forward) and 5′-CGCGGATCCCTACGAGTCGTCGTGGTTG-3′ (reverse), designed on the basis of the sequence of the PDEs from *L. major* (Accession No. XM_001682463.1). PCR amplifications were carried out using 600–800 ng of *L. donovani* genomic DNA, 100 ng of each primer, 2.5 mM $MgCl_2$, 0.2 mM dNTPs, and 1–2 units of Taq DNA polymerase (Invitrogen). Amplified DNAs were inserted between the *Nde*I and the *Bam*HI site of the pET16b plasmid and the sequence was confirmed. After transformation into *Escherichia coli* BL21 (DE3) pLysS, the protein was expressed according to standard procedures. Recombinant protein was isolated with Ni–nitrilotriacetic acid resin according to the manufacturer's (Qiagen, Germantown, NY, USA) recommendations.

PDE assay

PDE activity was assayed according to Schilling et al. [25]. All assays were performed at 30°C for 20 min in 25 mM Tris–HCl, pH 7.4, 0.5 mM EDTA, 0.5 mM EGTA, 10 mM $MgCl_2$ using [^{3}H]cAMP or [^{3}H]cGMP (50,000 dpm/reaction) as the substrate in a total volume of 100 μl. Reactions were stopped by adding 50 μl of 21.5 mM $ZnCl_2$, followed by 50 μl of 9 mM $Ba(OH)_2$, and incubated in ice for 30 min. The precipitates were filtered through GF/C glass fiber filters, and radioactivity was measured by scintillation spectrometry. For inhibitor studies, the test compounds were dissolved in PBS or dimethyl sulfoxide. The dimethyl sulfoxide concentration in the final assay solutions never exceeded 2%, and appropriate controls were always included.

Immunoblotting

Antibodies against LdPDEA and LdPDED were raised in rabbits using the recombinant protein expressed in *E. coli.* Antibodies against phosphodiesterase B (LdPDEB1 and 2), arginase (LdARG), ornithine decarboxylase (LdODC), cationic amino acid transporter (LdAAP3), polyamine permease (LdPOT1), and cytosolic tryparedoxin (LdCTRX) were raised in rabbits using peptides comprising the sequences of the respective proteins (NSNRAKWQEILDGRRDSIR for LdPDEB, GETLLYTPHTSSKGS for LdARG, PVYTREGNTLRCVSE for LdODC, LITPILEKSPGTPAY for LdAAP3, KWKAGHWPEVAKVIA for LdPOT1, and LTQDPEGAQFPWRDE for LdCTRX) and purified by Aminolink column (Pierce, Rockford, IL, USA) according to the manufacturer's protocol. Antibodies against topoisomerase II (LdTOPOII), ascorbate peroxidase (LmjAPX), and tryparedoxin peroxidase (LdTRXPX) were kind gifts from Dr. H.K. Majumder, Dr. Subrata Adak (Indian Institute of Chemical Biology, Kolkata), and Dr. Chandrima Shaha (National Institute of Immunology, New Delhi), respectively. Western blot analyses were performed as described earlier [13]. The primary antibodies were used with dilutions of 1:1000, and secondary antibodies (alkaline phosphatase conjugated) were used at a dilution of 1:10,000.

RT-PCR analysis

Total cell RNA was isolated using the RNAeasy kit (Qiagen). Five micrograms of total RNA was used to synthesize the first-strand cDNA with the SuperScript reverse transcriptase (Invitrogen). cDNAs were PCR-amplified with gene-specific primers as follows: LdPDEA, 5′-TTTCTGCAAAAATTCAAGATT-3′ (forward), 5′-AAATGTCGGCCATTTTCAGA-3′ (reverse); LdARG, 5′-ATGGAATACAAGGCTGGAGAG-3′ (forward), 5′-CCACGTGAGCGACAA-3′ (reverse); LdODC, 5′-GCCTCTACCACAGCTTCA-3′ (forward), 5′-CAGGCGCACAAACACAAG-3′ (reverse); LdPOT1, 5′-TGAAGAAGGTGAACTGGGC-3′ (forward), 5′-GAACTCCATGCTCACGCTAAA-3′ (reverse); LdAAP3, 5′-CTTCATGGTGCTGTATTTTGC-3′ (forward), 5′-GCCGCTGTACATCCAAAAGTA-3′ (reverse); LdAPX, 5′-AATGCCTGTATGCGGGTAACA-3′ (forward), 5′-CAAACGTCACTGGGAAGCAT-3′ (reverse); LdTRXPX, 5′-ATGTCCTGCGGTGACGCC-3′ (forward), 5′-TTACTTATTGTGATCGACCTTCAGGCC-3′ (reverse); LdCTRX, 5′-ATGTCCGGTGTCAGCAAGC-3′ (forward), 5′-TTACTCGTCTCTCCACGGAAA-3′ (reverse); LdHPRT, 5′-ATGAGCAACTCGGCCAAGT-3′ (forward), 5′-CTACACCTTGCTCTCCGGCTT-3′ (reverse).

Flow cytometry

Intracellular peroxide levels were determined by using the dye incorporation studies of Carter et al. [26], employing 2′,7′-dichlorodihydrofluorescein diacetate (H_2DCFDA). H_2DCFDA freely diffuses across cell membranes, is diacetylated, and incorporates into the cell [26]. After appropriate treatments, cells were exposed to the dye at a concentration of 20 μM for 15 min. The cells were then washed once with PBS by centrifugation at 5000 rpm for 5 min to remove extracellular H_2DCFDA, 50 μM H_2O_2 was added to the required cell groups, and the cells were kept in the dark for 5 min before readings were taken. For measurement of thiol content, promastigotes were incubated for 30 min with the thiol-reactive dye chloromethyl fluorescein diacetate (CMFDA) at 20 μM and washed once with PBS. The fluorescence levels of 50,000 cells were then counted for each condition using a FACSCalibur cytometer (BD Biosciences, San Jose, CA, USA). DIVA software (BD Biosciences) was used for data analysis for generation of histograms.

Arginase and ODC assays

Arginase was assayed as described by Corraliza et al. [27]. In brief, assays were initiated by the addition of 20 μl of parasite extract (2.5 mg protein/ml) to an 80-μl reaction mixture containing 25 mM Tris–HCl, 5 mM $MnCl_2$, pH 7.4. The mix was subsequently incubated at 56°C for 10 min for activation. Arginine hydrolysis was carried out by incubating 25 μl of the activated lysate with 25 μM arginine for 60 min at 25°C and the reaction was stopped with 400 μl of a mixture of H_2SO_4, H_3PO_4 and H_2O (1:3:7, v/v). The urea formed was measured at 540 nm after the addition of α-nitrosopropiophenone and subsequent heating at 100°C for 45 min. ODC was assayed as described by Hanson et al. [28]. In brief, ODC activity in promastigote extracts was measured by the amount of $^{14}CO_2$ released from 0.4 mM L-[1-^{14}C] ornithine (50 mCi/mmol) at 37°C and trapped in 200 μl of hyamine hydroxide. ODC activity was calculated as the mean nanomoles of $^{14}CO_2$ produced per milligram of protein extract over 1 h.

Uptake assays

The rates by which normal or PDEA-inhibited *L. donovani* promastigotes take up 20 μM [^{14}C]arginine (50 μCi/mmol) or [^{14}C] putrescine (50 μCi/mmol) were assayed by a previously described oil-stop method over various time intervals as indicated [29].

Immunofluorescence

L. donovani promastigotes were affixed to coverslips with 2% paraformaldehyde, washed three times with PBS, and incubated with anti-LdPDEA antibody (1:50) for 1 h at 4°C. Subsequently, cells were washed three times with PBS and probed with FITC-conjugated goat anti-rabbit secondary antibody (1:1000) for 1 h at 4°C. The promastigotes were preincubated with 4′,6-diamidino-2-phenylindole (DAPI; 1 μg/ml) at 22°C in PBS plus 10 μg/ml RNase A to label the nucleus and analyzed immediately. Images were captured using an Olympus BX61 microscope fitted with a DP71 digital camera and were processed using ImagePro Plus (Media Cybernetics, Bethesda, MD, USA).

Separation of thiols by high-pressure liquid chromatography (HPLC)

HPLC analysis of reduced thiols was carried out according to Mukhopadhyay et al. [7]. Ten milliliters of cell suspension (10^6/ml) in 50 mM Hepes (pH 8.0) containing 5 mM EDTA was taken in a dark tube and 0.1 ml of 2 mM monobromobimane in ethanol was added with mixing, and the suspension was incubated at 70°C for 3 min. The suspension was mixed with 0.2 ml of cold 25% trichloroacetic acid and incubated on ice for 20 min, after which denatured proteins and cell debris were removed by centrifugation. Samples were analyzed by HPLC using an ion-paired reversed-phase C18 column with a linear gradient of 0–90% methanol in 0.25% acetic acid (pH 3.5). Thiols were identified from bimane fluorescence with excitation at 360 nm and emission at 450 nm using an online fluorescence detector.

LdPDEA-overexpressing promastigotes

From *L. donovani* genomic DNA, the LdPDEA ORF was amplified using the primers 5′-CACCATGCTCGACTTTCTTGAGCAG-3′ (forward) and 5′-CTACGAGTCGTCGTGGTTG-3′ (reverse) and cloned in the pcDNA 3.1 directional TOPO expression vector (Invitrogen). The PDEA gene was then subcloned into the *Bam*HI and *Eco*RV-digested pTEX vector [30]. Promastigotes were transfected with ~20 μg of either vector alone (pTEX) or pTEX with the PDEA gene in the correct orientation (pTEXpdeA) by electroporation with a Gene Pulser (Bio-Rad, Hercules, CA, USA) under the conditions described earlier [13]. Transfectants were allowed to recover in drug-free medium for 24 h and were then selected for resistance to G418 at 25 and 50 μg/ml.

Knockdown construct for LdPDEA

The *L. tarentolae* T7.TR. strain (LtT7.TR; Jena Bioscience, Jena, Germany) has the T7 RNA polymerase and tetracycline-repressor genes integrated in the small ribosomal subunit locus and under the control of the antibiotics nourseothricin and hygromycin (100 μg/ml each). The vector pLew82v4 (kind gift from Professor G.A.M. Cross, The Rockefeller University, New York, NY, USA), which has a T7 promoter and a tet-operator sequence, was used. An antisense construct of LdPDEA was generated by cloning a segment from the 5′ terminus in reverse orientation into the *Hin*dIII and *Bam*HI sites of the pLew82v4 vector to construct pLewpdeA(as). The antisense construct was electroporated into the LtT7.TR promastigotes and selected using nourseothricin (100 μg/ml), hygromycin (100 μg/ml), and phleomycin (25 μg/m).

Results

Intracellular cAMP induces resistance to hydrogen peroxide and peroxynitrite

At the onset of mammalian infection, *L. donovani* promastigotes encounter a huge shift in temperature from 22°C in the insect gut to 37°C in the mammalian host and a shift of pH from 7.4 in sandfly gut to 5.5 in parasitophorous vacuoles of macrophages. We showed earlier that exposure to such temperature and pH renders the promastigotes more resistant to H_2O_2 and peroxynitrite ($ONOO^-$) and this was associated with an increase in intracellular cAMP level [13]. Similar to stress exposure, resistance to both H_2O_2 and $ONOO^-$ was increased when promastigotes were pretreated with cell-permeative cAMP analogues, 8-(4-chlorophenylthio)-cAMP (pCPTcAMP) and 8-bromo-cAMP (8-BrcAMP). These derivatives differ considerably in their lipophilicity and intracellular stability, i.e., resistance to cellular cAMP–PDE-mediated degradation. pCPTcAMP was found to induce resistance against oxidants as the percentage of control viability increased by 23.4 ± 2.2 and 19.2 ± 1.9% against 250 μM H_2O_2 and 400 μM $ONOO^-$, respectively, in pCPTcAMP-treated cells compared to normal cells (Fig. 1A). A weaker effect was seen with the less lipophilic and less stable derivative 8-BrcAMP as the percentage control viability increased by 14.2 ± 1.2 and 12.4 ± 1.0% against 250 μM H_2O_2 and 400 μM $ONOO^-$, respectively, in 8-BrcAMP-treated cells (Fig. 1A). To further ascertain the ability of these cAMP analogues to induce the peroxide-neutralization capacity of promastigotes, a FACS cell analysis was employed using the H_2O_2-reactive green fluorescent dye H_2DCFDA. Promastigotes were treated with H_2DCFDA for 15 min, washed in PBS, and exposed to H_2O_2 and then

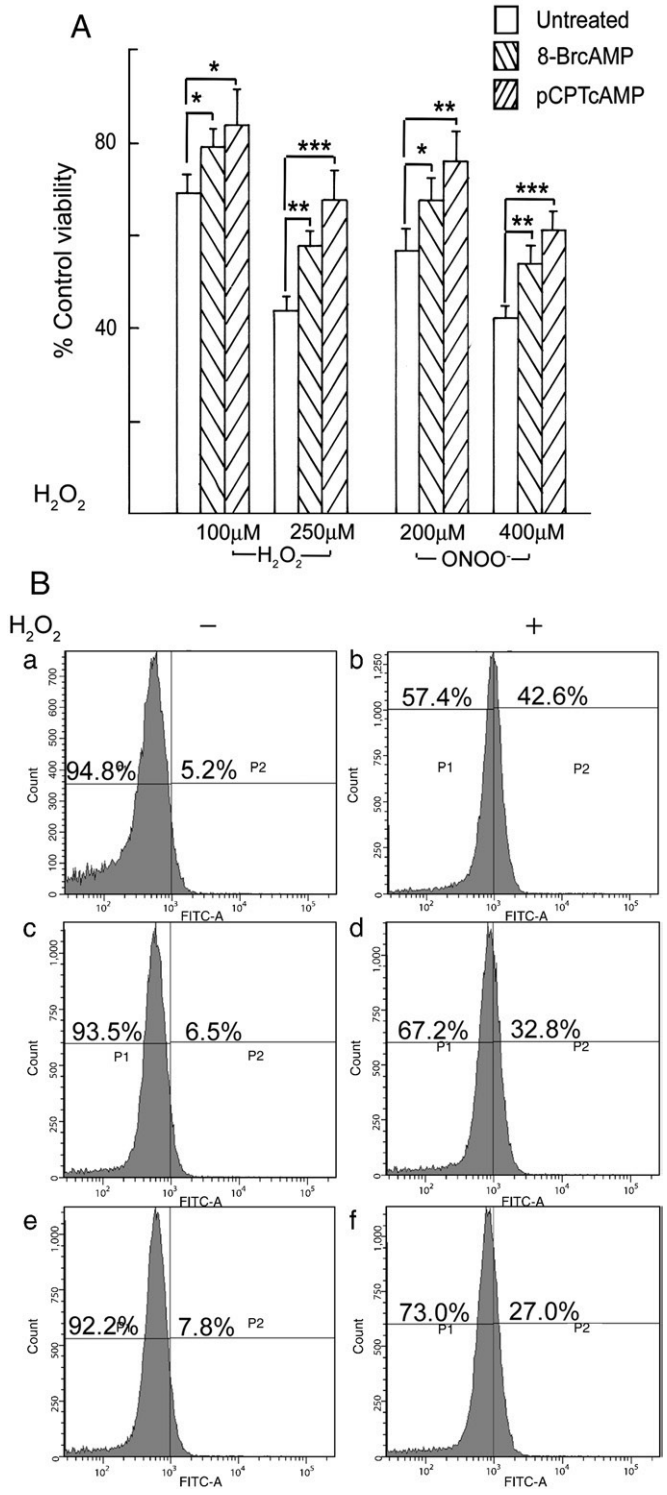

Fig. 1. Role of intracellular cAMP in resistance to oxidative damage. (A) Promastigotes pretreated with 8-BrcAMP (500 μM) or pCPTcAMP (500 μM) for 12 h were exposed to H_2O_2 and ONOO− for 1 h and 15 min, respectively. Viability was measured according to their conversion of the dye MTT to formazan, a function that depends on mitochondrial activity. Data are presented as means ± SD ($n=3$). ***$p<0.001$, **$p<0.01$, and *$p<0.05$ vs control. (B) pCPTcAMP (500 μM)- and 8-BrcAMP (500 μM)-treated cells were incubated with H_2DCFDA. The cells were subsequently exposed to H_2O_2, and representative histograms plotting the fluorescence levels of 50,000 cells are shown (a–f). The lower boundary of the P1 gate defines the cutoff for an event to be registered as cellular fluorescence, whereas the P2 gate was established to measure population shifts and delineate approximately the upper 5% of the fluorescence boundary of normal untreated cells. (a) Untreated cells, P2 = 5.2 ± 0.4%; (b) H_2O_2-exposed cells, P2 = 42.6 ± 4.0%; (c) 8-BrcAMP-treated cells, P2 = 6.5 ± 0.5%; (d) 8-BrcAMP-treated and H_2O_2-exposed cells, P2 = 32.8 ± 3.1%; (e) pCPTcAMP-treated cells, P2 = 7.8 ± 0.6%; (f) pCPTcAMP-treated and H_2O_2-exposed cells, P2 = 27.0 ± 2.5%.

the fluorescence levels of 50,000 cells were counted. A gate (P2) was established that delineated the upper 5% of fluorescent cells. The percentages of gated cells were 11.1 ± 1.0 and 18.2 ± 1.7% ($n=4$) higher in normal promastigotes compared to promastigotes pretreated with 8-BrcAMP and pCPTcAMP, respectively (Fig. 1B). Here also, a weaker effect was observed with 8-BrcAMP than with pCPTcAMP, indicating that neutralization of H_2O_2 may be directly related to intracellular cAMP level.

Differential expression of PDEA in the life cycle of L. donovani

Because the intracellular cAMP pool is regulated in part by cAMP-specific PDEs, we thought it worthwhile to study the status of PDE in *L. donovani*. cAMP-PDE activity remained mostly unaltered in the membrane and microsomal fractions, whereas in the cytosolic fraction it diminished gradually as the parasite differentiated from log phase to the axenic amastigote stage (reduction of 11.9 ± 1.9, 19.0 ± 1.0, and 49.8 ± 2.5%, respectively, in early stationary, late stationary, and axenic amastigote stages compared to log-phase promastigotes; Fig. 2A). Each subcellular fraction was characterized by Western blotting against marker proteins, namely, binding protein (LdBiP) for the microsomal, amino acid permease (LdAAP3) for the membrane, and tryparedoxin peroxidase (LdcTRX) for the cytosolic fraction (Supplementary Fig. S1). Because the total PDE activity was markedly diminished in the cytosolic fraction of amastigotes, we analyzed the expression of various forms of PDE at the protein level in different stages of the *L. donovani* life cycle by Western blot analysis using polyclonal antibodies against LdPDEs. As shown in Fig. 2B, PDEA was significantly depleted in late stationary-phase promastigotes (~2.2-fold) and axenic amastigotes (~2.5-fold) compared to log-phase promastigotes. Though the expression of other PDEs such as PDEB and PDED remained mostly unaltered, subtle differences in the protein levels of PDEB and PDED were detected between log-phase and early stationary-phase promastigotes. However, such differences seemed insignificant, as similar differences were detected for Ld topoisomerase II, a protein expressed equally in all life-cycle stages of the parasite and used as a control in this experiment [31] (Fig. 2B). A kinetic analysis for PDEA, carried out by Western blotting using cell-free extracts of promastigotes exposed to differentiation conditions (37°C and pH 5.5), revealed gradual reduction of PDEA levels with increased time of exposure (1.5-fold for 3 h, 2.1-fold for 6 h, and 4.0-fold for 12 h exposure) (Fig. 2C). The intracellular PDEA level was further examined by immunofluorescence analysis of promastigotes exposed to differentiation conditions using anti-LdPDEA antibody and FITC-conjugated anti-rabbit secondary antibody (Fig. 2D). Cells were stained with DAPI to label nuclear and kinetoplast DNA and the number of FITC-positive cells was expressed as a percentage of the DAPI-positive cells. As depicted in Fig. 2E, FITC-positive cells were reduced to 48.3 ± 3.3, 30.4 ± 2.6, and 23.1 ± 2.0% in promastigotes exposed to differentiation conditions for 3, 6, and 12 h, respectively. Taken together, these results suggest a differential expression and a gradual reduction of PDEA level during the course of differentiation from promastigote to amastigote.

Cloning and characterization of LdPDEA

The *Leishmania* genome suggests the existence of at least four different cAMP-PDEs of which PDEA is putatively cytosolic, whereas PDEs B1 and B2 are located in flagella and the FYVE domain containing PDEC is essentially membrane-associated. We amplified the complete ORF of PDEA from the *L. donovani* genome and cloned it in the bacterial vector pET16b and expressed it in *E. coli* as a His-tagged recombinant protein (rLdPDEA) (Supplementary Fig. S2). A search for conserved domains suggested PDEA to be a typical class I PDE with a C-terminal catalytic domain (PDEase I) and metal-binding HDc domain (Fig. 3A). Analysis of amino acid sequence suggested PDEA

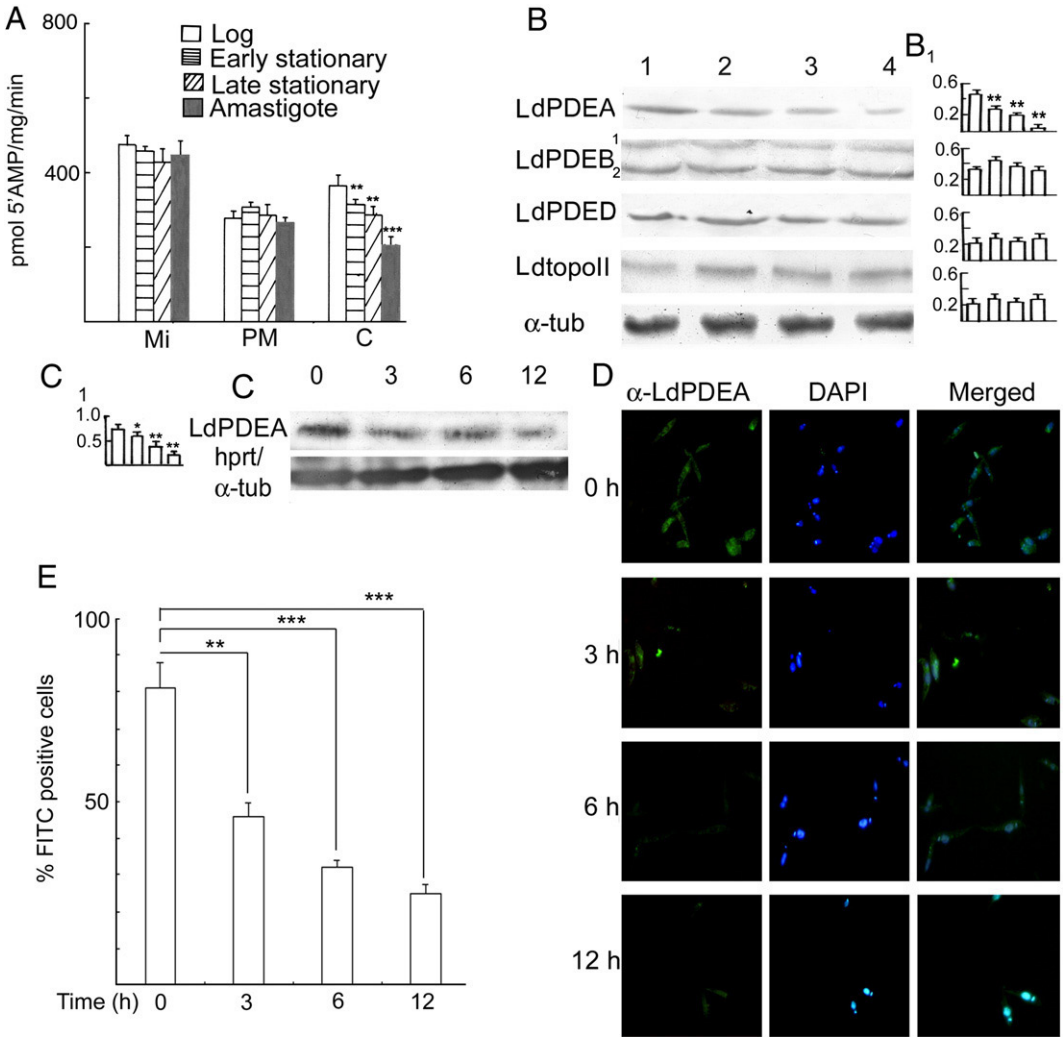

Fig. 2. Distribution of PDE in various life stages. (A) Cell-free extracts prepared from various morphotypes of *L. donovani* were subjected to differential centrifugation to obtain microsomal (Mi), plasma membrane (PM), and cytosolic (C) fractions. Each fraction from each of the morphotypes was assayed for PDE activity using 5 mM $MgCl_2$ and 50 μM cAMP. Values are means ± SD ($n = 3$). ***$p<0.001$ and **$p<0.01$ vs log-phase promastigotes. (B) Immunoblot analysis of various forms of PDE from cell-free extracts of log-phase promastigotes (lane 1), early stationary-stage promastigotes (lane 2), late stationary-stage promastigotes (lane 3), and axenic amastigotes (lane 4) using antibodies against the respective proteins. LdTOPOII was analyzed as a control for stage-specific expression and α-tubulin was used as an endogenous control. (C) Immunoblot analysis of PDEA in *L. donovani* promastigotes at various time points after exposure to differentiation conditions. Results are representative of duplicate samples of three separate experiments and the densitometric evaluations are the means of three separate experiments. **$p<0.01$ vs log-phase promastigotes (B_1) and **$p<0.01$, *$p<0.05$ vs 0 h (C_1). (D) Immunofluorescence analysis of intracellular PDEA in *L. donovani* promastigotes by anti-LdPDEA antibody probed with FITC-conjugated goat anti-rabbit secondary antibody at various time points after exposure to differentiation conditions. Nuclei and kinetoplast were visualized by DAPI staining. (E) 200 separate fields were scanned to score the number of FITC-positive cells against DAPI-positive cells to calculate the percentage of FITC positives in each time point. ***$p<0.001$ and **$p<0.01$ vs 0 h.

to be highly conserved in common *Leishmania* species (>80% identity) and that it has orthologues in both *T. cruzi* (49.0% identity) and *T. brucei* (44.0% identity) (Figs. 3A and B). Based on its amino acid sequence, PDEA is only ~38% identical with the human enzyme (HsPDE4B). Analysis of the active-site sequence revealed a single mismatch of a catalytically insignificant histidine residue (H^{478} in HsPDE4B) replaced by leucine (L^{459} in the corresponding position; Table 1). Two residues conferring selectivity for cAMP over cGMP (Q^{443} and N^{567} in HsPDE4B) are also conserved in corresponding positions in LdPDEA. The bacterially expressed protein showed a K_M of 166.66 μM (Fig. 3C). Immunolocalization analysis was carried out in log-phase promastigotes using anti-LdPDEA antibody to probe PDEA and DAPI to stain nuclear and kinetoplast DNA. As shown in Fig. 3D, the signal for PDEA was distributed throughout the cell but did not colocalize with DAPI-stained nuclei or kinetoplast, indicating cytosolic localization of PDEA (Fig. 3D). Immunoblot analysis of subcellular fractions also revealed predominant cytosolic localization with very poor signals in membrane and microsomal fractions (Supplementary Fig. S1). Although the Ca^{2+} chelator EGTA had no effect, the Mg^{2+} chelator EDTA caused an irreversible inactivation of the enzyme at all concentrations used (maximum inhibition of 64.4 ± 5.7% of total PDE activity at 20 mM EDTA), indicating a requirement for Mg^{2+} for the active conformation (Fig. 3E). The activity of the enzyme was not stimulated by Ca^{2+} (1–200 μM) or by Ca^{2+} calmodulin (Supplementary Fig. S3). Furthermore, the enzyme was not able to hydrolyze cGMP at a broad range of concentrations (1 nM–10 mM) and cGMP had no effect either on the substrate affinity or on cAMP hydrolytic activity (results not shown). All these results suggest that LdPDEA is a cAMP-specific cytosolic PDE not regulated by cGMP.

Resistance against H_2O_2 when PDEA activity was blocked

A panel of PDE inhibitors was tested against rLdPDEA, of which etazolate ($IC_{50} = 19.3 \pm 1.6$ μM), trequinsin ($IC_{50} = 28.5 \pm 2.1$ μM), and dipyridamole ($IC_{50} = 23.4 \pm 1.1$ μM) exhibited maximum inhibitory activity (Table 2). Interestingly, in contrast to its trypanosomal orthologues (TcPDEA and TbPDEA), LdPDEA showed moderate sensitivity to the nonselective mammalian PDE inhibitor IBMX

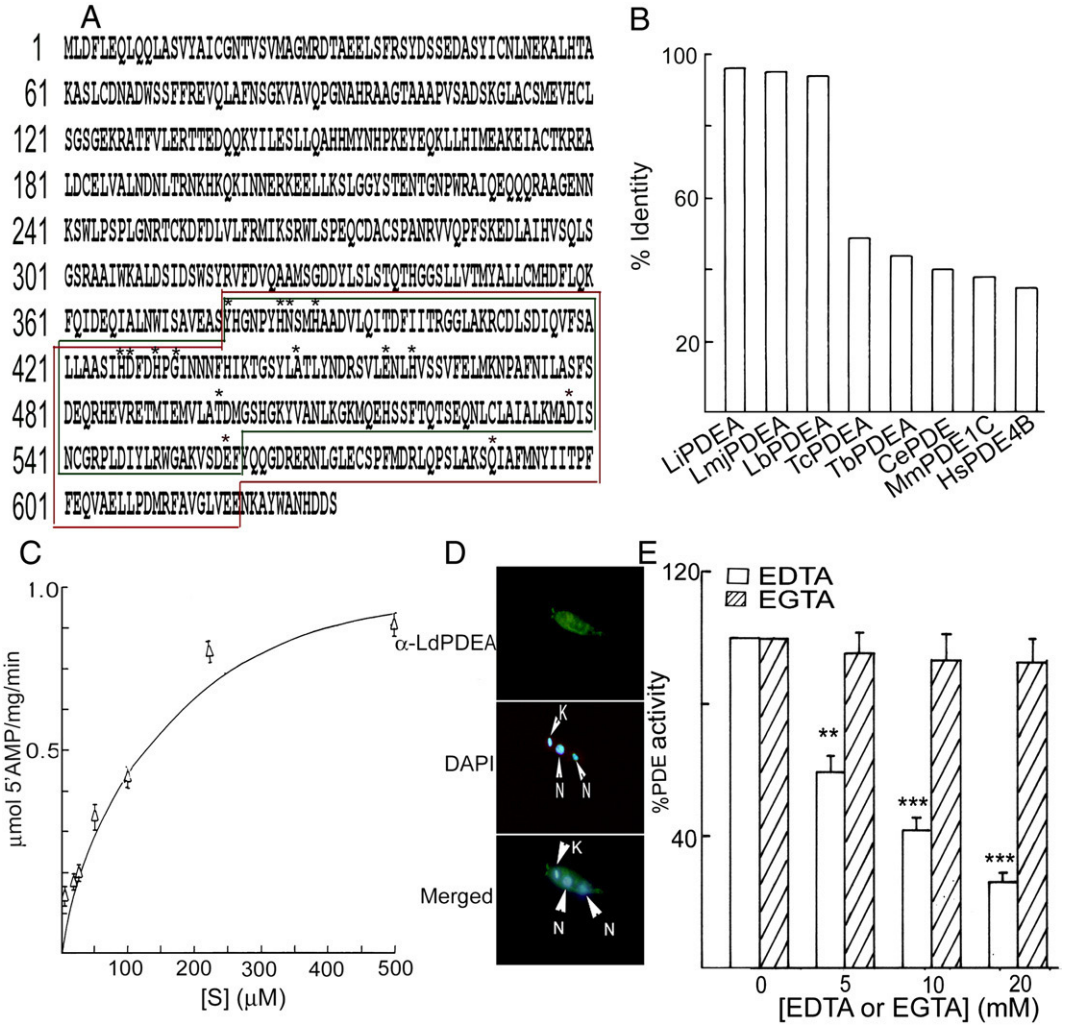

Fig. 3. Characterization of recombinant LdPDEA. (A) Predicted amino acid sequence of LdPDEA. Metal-binding HDc domain (green) and PDEase I catalytic domain (red) are boxed. Asterisks denote amino acids that are conserved in most class I cAMP PDEs. (B) Amino acid sequence identity of LdPDEA with class I PDEs from a diverse group of organisms: Li, *Leishmania infantum;* Lmj, *Leishmania major;* Lb, *Leishmania braziliensis;* Tc, *Trypanosoma cruzi;* Tb, *Trypanosoma brucei;* Ce, *Caenorhabditis elegans;* Mm, *Mus musculus;* Hs, *Homo sapiens.* (C) Michaelis–Menten kinetics of LdPDEA indicates a K_M of 166.66 µM for cAMP. (D) Intracellular localization of LdPDEA. Log-phase promastigotes were fixed and incubated with anti-LdPDEA antibody for 1 h at 4°C and subsequently probed with FITC-conjugated secondary antibody. Promastigotes were preincubated with DAPI to label nuclei and kinetoplast. (E) Mg^{2+} dependence of LdPDEA activity was examined by preincubating the enzyme for 30 min with the indicated concentrations of EDTA or EGTA. The enzyme solutions were then diluted 1250× into standard reaction buffer and PDE activities were determined. Data are presented as a percentage of hydrolysis in two separate experiments done in triplicate, values are means ± SD. ***$p<0.001$, **$p<0.01$ vs no EDTA or EGTA (defined as 100% activity).

(IC_{50} = 57.0 ± 4.2 µM) (Table 2). Dipyridamole is also a potential inhibitor of PDEB, the major cAMP PDE of the parasite (IC_{50} = 29 µM). Etazolate and trequinsin also showed moderate inhibitory activity against PDEB (IC_{50} > 100 µM for etazolate and IC_{50} = 96 µM for trequinsin) [22]. To ascertain the functional significance of LdPDEA, we, therefore, treated log-phase promastigotes with etazolate and trequinsin. These inhibitors did not have any toxic effects on the growth of *L. donovani* promastigotes at concentrations higher than the IC_{50} values during a course of 12 h treatment (etazolate up to 30 µM and trequinsin up to 39 µM, data not shown). Log-phase *L. donovani* promastigotes treated with etazolate (25 µM) and trequinsin (30 µM) exhibited 24.2 ± 2.4 and 22.0 ± 1.5% higher resistance against H_2O_2 (n = 3), respectively, and 11.4 ± 1.0 and 13.2 ± 0.9% higher resistance against $ONOO^-$ (n = 3) compared to untreated promastigotes as determined by cell viability. However, because these inhibitors are not specific for PDEA, the effects of their treatment might be due to simultaneous inhibition of more than one form of PDE in *L. donovani* promastigotes. A knockdown construct was therefore prepared in the pLEW82v4 plasmid with the T7 polymerase promoter and PDEA in the antisense orientation. It was transfected into *L. tarentolae* with chromosomally integrated genes for T7 RNA polymerase and a tetracycline repressor (LtT7.TR) to build up a tetracycline-inducible PDEA knockdown system. After tetracycline induction, PDEA expression was strongly diminished at both the RNA and the protein level (Fig. 4A, inset). These cells looked completely normal and proliferated well as long as they were kept in continuous

Table 1
Amino acid replacements of conserved residues in the catalytic domains of LdPDEA

HsPDE4B	Y^{399}	H^{406}	N^{407}	H^{410}	H^{446}	D^{447}	H^{450}	G^{452}	A^{466}	E^{476}	H^{478}	H^{479}	T^{517}	D^{564}	E^{585}	Q^{615}
LdPDEA	–	–	–	–	–	–	–	–	–	–	L^{459}	–	–	–	–	–

Amino acid conservation is indicated by dash.

Table 2
Effects of various inhibitors on LdPDEA

Inhibitor	IC_{50} (μM) human PDE	IC_{50} (μM) LdPDEA	Range applied (μM)
IBMX	Nonspecific	57.0 ± 4.2	5–500
Etazolate	2.0	19.3 ± 1.6	0.5–100
Rolipram	2.0	230.0 ± 17.3	0.5–500
Dipyridamole	0.38	23.4 ± 1.1	0.5–100
Theophylline	50–300	>100	50–500
EHNA	1.0	>100	0.5–200
Zardeverine	0.5	140.2 ± 11.0	0.5–300
Trequinsin	0.003	28.5 ± 2.1	0.5–100
Papaverine	5–25	62.3 ± 5.7	5–200
Zaprinast	0.5	Not detectable	5–500

culture (Fig. 4A). LtT7.TR cells bearing pLewpdeA(as) showed 21.9 ± 2.0 and 13.1 ± 1.2% enhanced resistance against H_2O_2 and $ONOO^-$, respectively ($n = 3$), after PDEA knockdown by tetracycline induction (Fig. 4B). To determine peroxide neutralization capacity of PDEA-silenced or inhibited cells, a FACS-based approach using H_2DCFDA was employed as described earlier. The percentage of gated cells was 15.0 ± 0.9 and 12.9 ± 1.0% higher in normal cells exposed to H_2O_2 than in etazolate- and trequinsin-treated cells, respectively (Fig. 4C). On induction of PDEA silencing by tetracycline, transfected cells were able to neutralize H_2O_2 more efficiently, as the percentage of gated cells (10.5 ± 1.0%) was 12.9 ± 1.4% lower ($n = 5$) than in uninduced cells (23.4 ± 2.0%) (Fig. 4D). These results suggest that inhibition of PDEA either by chemical inhibitors or by gene silencing led to an enhanced H_2O_2 neutralization.

Effects of PDEA inhibition on TSH metabolism

As the peroxidase system in *Leishmania* is dependent on TSH, we wanted to study the effects of PDEA on TSH metabolism. No significant alterations in arginine and putrescine uptake nor in arginine and polyamine transporter expression were detectable in log-phase promastigotes after 12 h treatment of etazolate (25 μM) and trequinsin (30 μM) or in tetracycline-induced PDEA knocked-down Lt.T7TR cells (Supplementary Fig. S4). Parasite-encoded arginase attains its importance in parasite infectivity and disease outcome by subverting arginine away from inducible nitric oxide synthase [32].

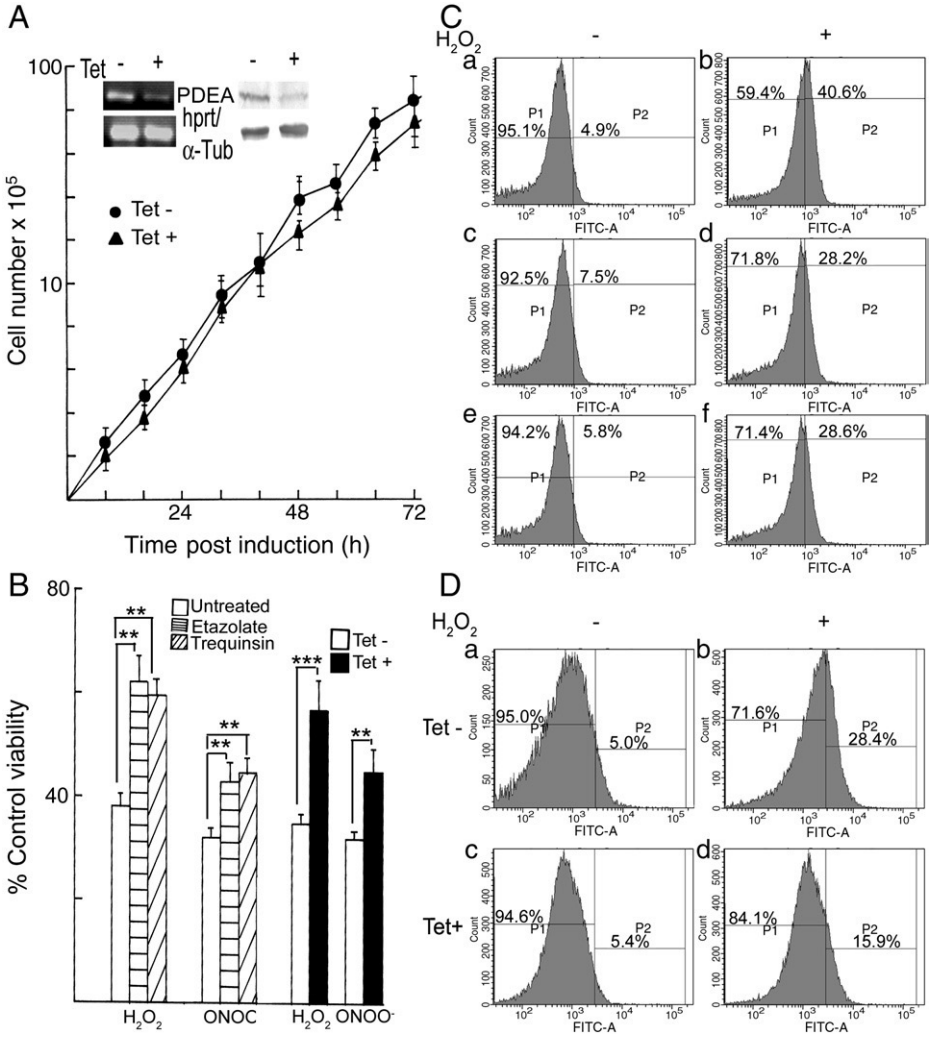

Fig. 4. Effect of PDEA inhibition on promastigote resistance against oxidative damage. (A) The effect of PDEA knockdown on parasite growth was assessed by growing the cells for 3 days after tetracycline induction. Cell number was determined every 8 h using a hemocytometer. PDEA was analyzed in cells 24 h postinduction by both RT-PCR and Western blotting to determine the knockdown efficiency (inset). (B) Promastigote viability against H_2O_2 and $ONOO^-$ was assayed after treatment with various PDE inhibitors and also after knocking down PDE. Values are means ± SD. ***$p<0.001$, **$p<0.01$ vs untreated control. (C) Representative histograms plotting the fluorescence of 50,000 cells treated with H_2DCFDA as described in the legend to Fig. 1. (a) Untreated cells, P2 = 4.9 ± 0.5%; (b) H_2O_2-exposed cells, P2 = 40.6 ± 3.9%; (c) etazolate (25 μM)-treated cells, P2 = 7.5 ± 0.6%; (d) etazolate-treated cells exposed to H_2O_2, P2 = 28.2 ± 2.8%; (e) trequinsin (30 μM)-treated cells, P2 = 5.8 ± 0.5%; (f) trequinsin-treated cells exposed to H_2O_2, P2 = 28.6 ± 2.6%. (D) Representative histograms of similar experiments with LtT7.TR cells bearing pLewpdeA(as) with or without tetracycline induction. (a) Uninduced cells, P2 = 5.0 ± 0.5%; (b) uninduced cells exposed to H_2O_2, P2 = 28.4 ± 2.5%; (c) tetracycline-induced cells, P2 = 5.4 ± 0.5%; (d) tetracycline induced and H_2O_2-exposed cells, P2 = 15.9 ± 1.5%.

N^{ω}-hydroxy-L-arginine (LOHA), a specific inhibitor of arginase, blocks intracellular proliferation of *Leishmania* by inhibiting parasite-encoded arginase [33]. ODC is another biosynthetic enzyme associated with parasitic virulence, and the irreversible ODC inhibitor difluromethylornithine (DFMO) can block proliferation of *Leishmania* promastigotes [34]. To determine the effects of PDEA on TSH biosynthesis, arginase and ODC activities were assayed in cells treated with etazolate (25 μM) and trequinsin (30 μM). As shown in Fig. 5A and B, both arginase and ODC activities were significantly increased ($p<0.01$, $n=4$) when cells were treated with etazolate (25 μM) (~1.4- and ~2.0-fold for arginase and ODC, respectively) and trequinsin (30 μM) (~1.4- and ~1.6-fold for arginase and ODC, respectively) for 12 h. In PDEA knocked-down cells also, arginase and ODC activities were significantly (~1.9- and ~1.6-fold for arginase and ODC, respectively, $p<0.01$, $n=5$) elevated compared to tetracycline-uninduced cells (Figs. 5C and D). Specificity of each of the assays was determined using LOHA and DFMO. The expression of arginase and ODC was also significantly increased at the protein level in etazolate-treated cells (~3.1- and ~1.6-fold for arginase and ODC, respectively) and in tequinsin-treated cells (~2.8- and ~1.9-fold for arginase and ODC, respectively) (Fig. 5E). In LtT7TR cells, selective PDEA silencing resulted in an elevation of arginase (~2.3-fold compared to tetracycline-uninduced cells) and ODC (~2.1-fold compared to tetracycline-induced cells) (Fig. 5F). These results indicate that inhibition of PDE activity could upregulate arginase and ODC activity of the parasite, which might affect the TSH pool by enhancing polyamine biosynthesis.

Effects of PDEA inhibition on the TSH pool

Because an upregulation of arginase and ODC is associated with PDE inhibition, we wanted to determine the total intracellular thiol content under such conditions. For this, a FACS approach was employed using CMFDA. Cells were treated with either etazolate (25 μM) or trequinsin (30 μM) for 12 h and incubated with the thiol-conjugating dye CMFDA before analysis of fluorescence. A gate (P2) was established that delineated the upper 5% of the fluorescent cells. The percentage of cells in the P2 gate was slightly higher for etazolate (increase of $3.7\pm0.3\%$, $n=4$)- and trequinsin (increase of $5.7\pm0.4\%$, $n=4$)-treated cells compared to untreated cells (Fig. 6A). PDEA knocked-down Lt.T7TR cells induced with tetracycline had only slightly increased content of reduced thiol, as the percentage of cells in the P2 gate was a little higher ($4.3\pm0.4\%$, $n=4$) compared to uninduced cells (Fig. 6B). To determine the TSH content of the parasite,

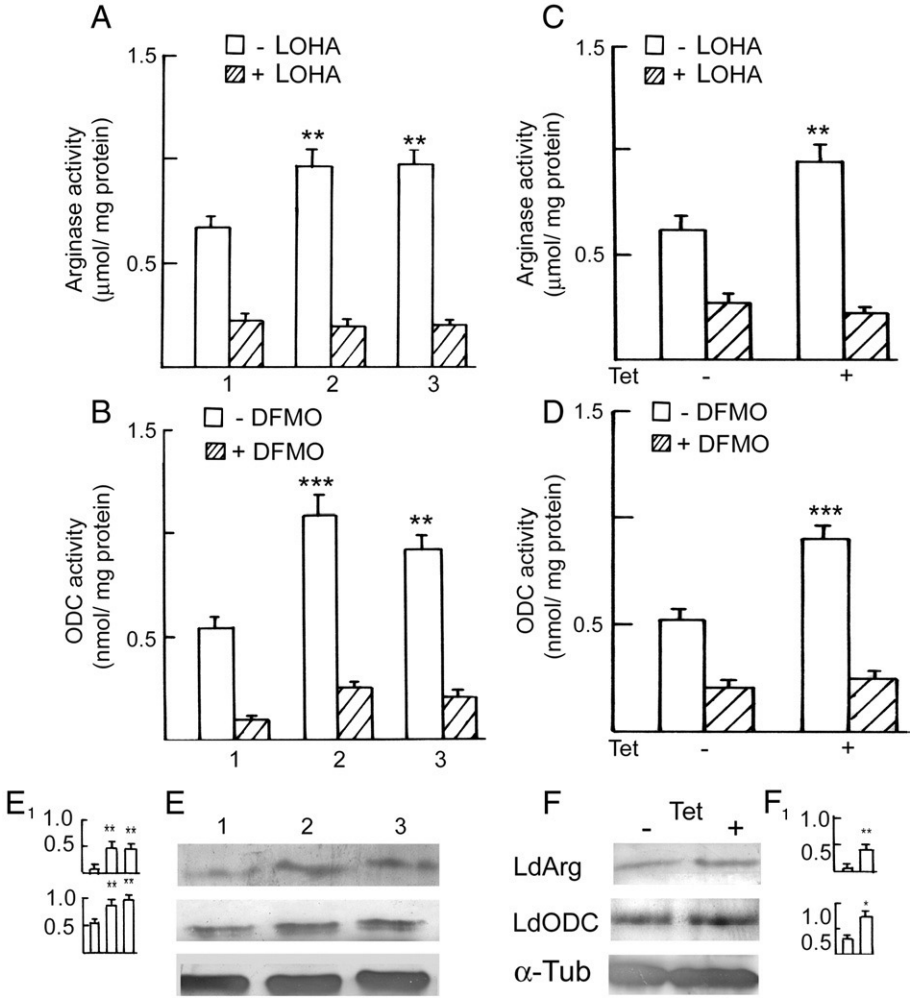

Fig. 5. Effects of PDEA inhibition on arginase and ODC activity. (A) Arginase and (C) ODC activities in extracts of untreated (columns 1), etazolate (25 μM)-treated (columns 2), and trequinsin (30 μM)-treated (columns 3) promastigotes, as measured over a 15-min time frame. Cell-free extracts from LtT7.TR cells bearing the pLewpdeA(as) plasmid were assayed for (B) arginase and (D) ODC activities with or without tetracycline induction. Data are represented as means ± SD ($n=4$ for inhibition and $n=5$ for silencing). ***$p<0.001$, **$p<0.01$ vs untreated cells. (E) Expression of arginase and ODC was analyzed by immunoblot analysis of the protein levels using antibodies against peptides comprising sequences corresponding to the respective proteins. (Lanes 1) Untreated, (2) etazolate (25 μM)-treated, and (3) trequinsin (30 μM)-treated cells. (F) Expression of the genes was analyzed by immunoblotting in tetracycline-induced and uninduced LtT7.TR cells bearing pLewpdeA(as). Band intensities were analyzed by densitometry (E_1 and F_1). α-Tubulin was used as an internal control. Results are representative of duplicate samples of three separate experiments and the densitometric evaluations are the means of three independent experiments; **$p<0.01$, *$p<0.05$ vs untreated cells.

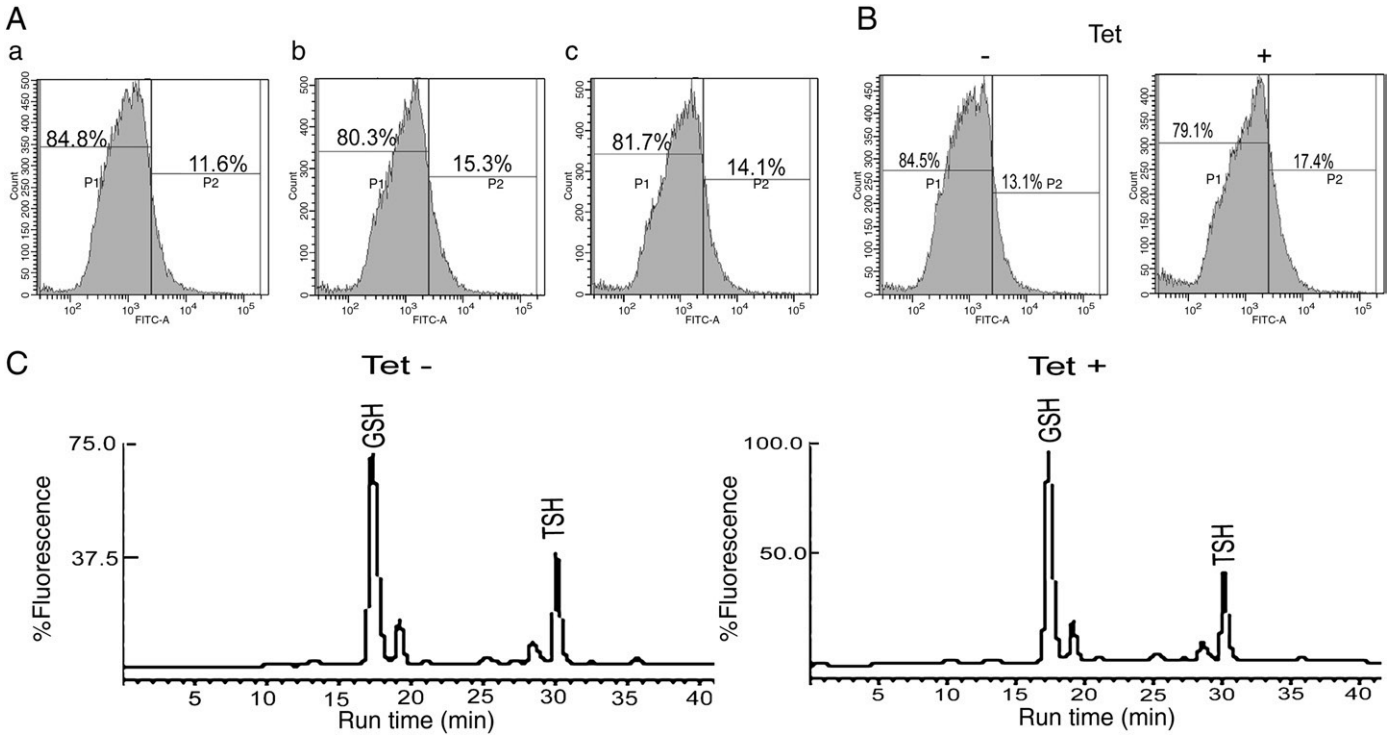

Fig. 6. Effect of PDEA inhibition on thiol content. (A) Representative histograms plotting the fluorescence of 50,000 cells treated with 20 μM CMFDA as described in the legend to Fig. 1. (a) Untreated cells, P2 = 11.6 ± 0.8%; (b) etazolate (25 μM)-treated cells, P2 = 15.3 ± 1.1%; (c) trequinsin (30 μM)-treated cells, P2 = 17.3 ± 1.2%. (B) Representative histograms for similar experiments with LtT7.TR cells bearing pLewpdeA(as) with or without tetracycline induction. (C) HPLC traces showing levels of reduced thiols (TSH and GSH) derivatized with monobromobimane in LtT7.TR promastigotes bearing pLewpdeA(as) with or without tetracycline induction. Peaks representing reduced thiols were identified using a control run of purified derivatized compounds.

reduced thiols were derivatized with monobromobimane and separated by reverse-phase HPLC and detected as peaks of fluorescence (Fig. 6C). Genetic silencing of PDEA did not significantly alter the level of TSH (increase of 3.9%, $n = 3$) in LtT7TR cells. These data suggest that even though PDEA inhibition caused an increase in arginase and ODC activity, this was not reflected in the TSH content of the parasite.

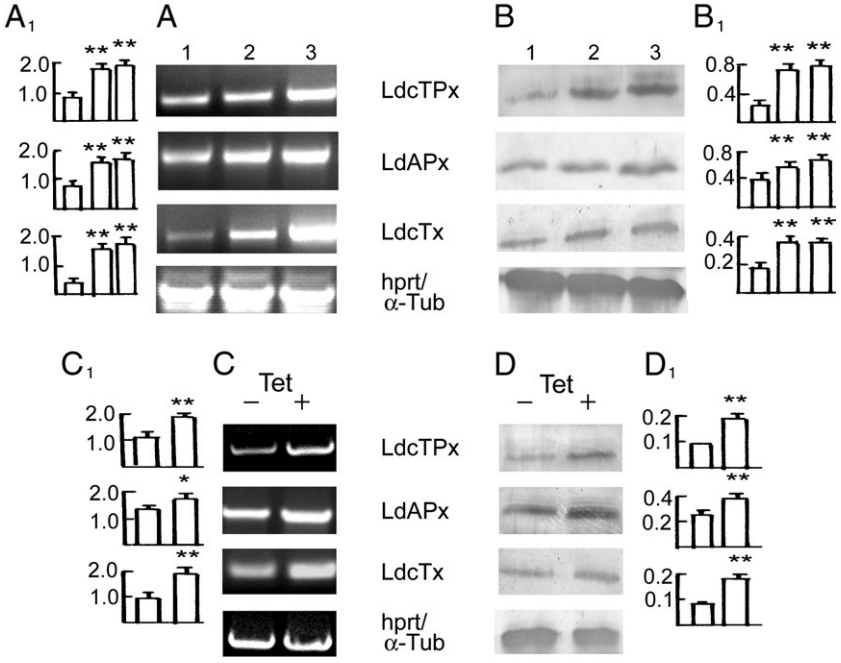

Fig. 7. Effects of PDEA inhibition on the trypanothione peroxidase system. The expression of tryparedoxin peroxidase (LdcTPx), ascorbate peroxidase (LdAPx), and tryparedoxin (LdcTx), comprising the cytosolic trypanothione peroxidase system, was analyzed by (A) RT-PCR and (B) Western blotting. (Lanes 1) Untreated, (2) etazolate (25 μM)-treated, and (3) trequinsin (30 μM)-treated cells. (C) RT-PCR and (D) Western blot analysis of the same genes in LtT7.TR cells bearing the pLewpdeA(as) plasmid with or without tetracycline induction. Hypoxanthine–guanine phosphoribosyltransferase (hprt) and α-tubulin were used as internal controls. Band intensities were analyzed by densitometry (A_1, B_1, C_1, and D_1). Results are from duplicate samples of three separate experiments and the densitometric evaluations are the means of three independent experiments; $^{**}p<0.01$, $^{*}p<0.05$ vs untreated cells.

TSH pool utilization when PDEA activity was blocked

Because PDE inhibitors caused enhanced peroxide neutralization, we, therefore, wanted to determine the status of tryparedoxin peroxidase and ascorbate peroxidase under PDE-inhibited conditions. mRNA analysis by semiquantitative RT-PCR and Western blotting by polyclonal antibodies showed significant upregulation of trypanothione peroxidase (~2.5-fold) and ascorbate peroxidase (~1.5-fold) in etazolate- and trequinsin-treated cells. A 2-fold increase in the cytosolic tryparedoxin level was also observed in inhibitor-treated cells (Figs. 7A and B). Moreover, selective PDEA silencing in Lt.T7TR cells also resulted in an ~2-fold increase in the levels of all three proteins (Figs. 7C and D). These results suggest that PDEA inhibition results in increased expression of cytosolic tryparedoxin and

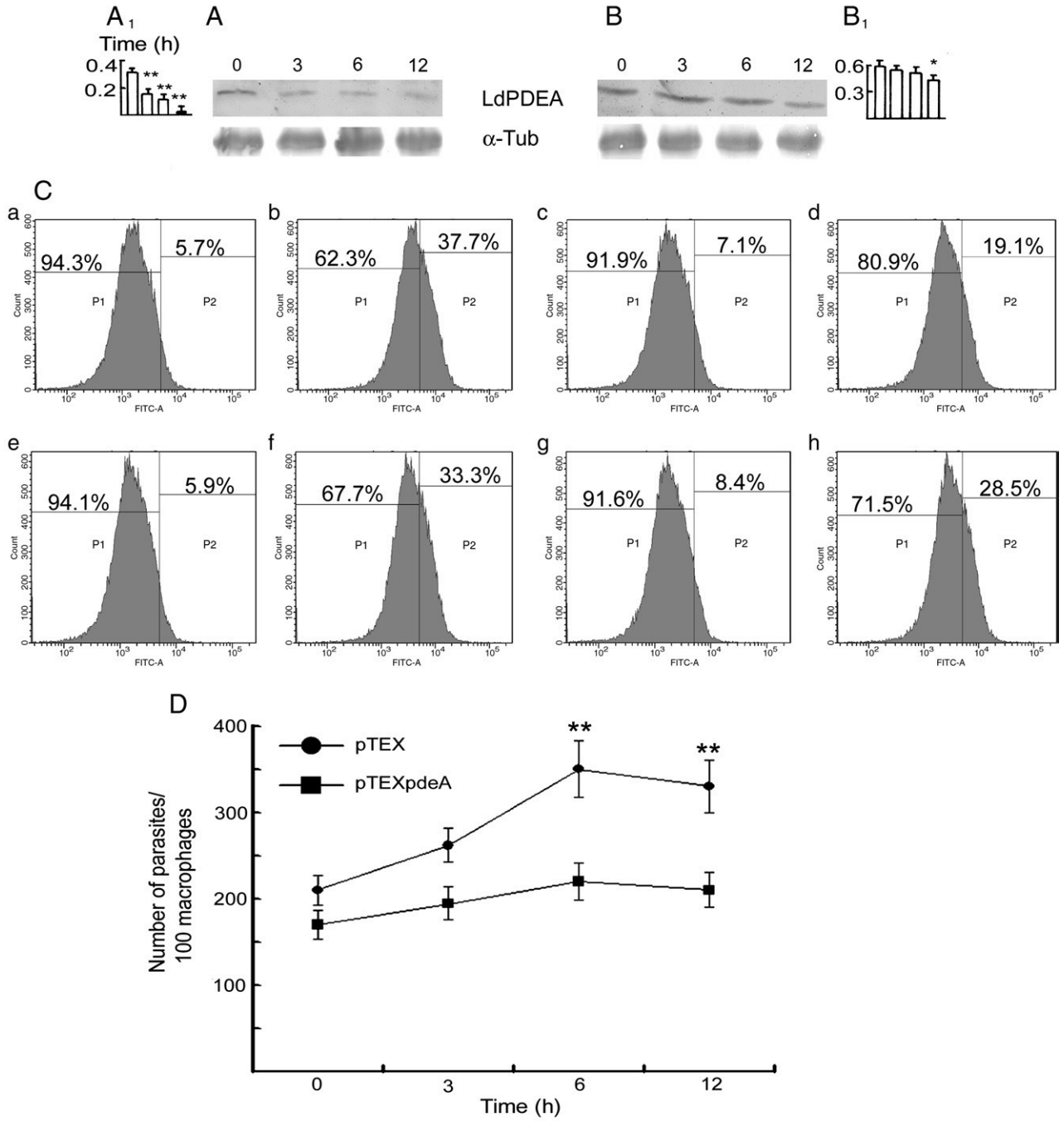

Fig. 8. Effects of LdPDEA overexpression on resistance against oxidative damage. (A and B) Western blot analyses of PDEA gene expression with anti-LdPDEA antibody at various time points after promastigotes were exposed to differentiation conditions (37°C and pH 5.5). Promastigotes were transfected (A) with empty vector or (B) with vector containing LdPDEA. Band intensities were analyzed by densitometry (A_1 and B_1). $^{**}p<0.01$, $^{*}p<0.05$ vs untreated cells. (C) Representative histograms plotting the fluorescence of 50,000 cells treated with H_2DCFDA as described earlier. (a) Cells bearing empty vector, P2 = 5.7 ± 0.5%; (b) cells bearing empty vector and exposed to H_2O_2, P2 = 37.7 ± 3.5%; (c) cells bearing empty vector and preincubated under differentiation conditions for 12 h, P2 = 7.1 ± 0.5%; (d) cells bearing empty vector, preincubated under differentiation conditions, and exposed to H_2O_2, P2 = 19.1 ± 1.9%; (e) cells bearing vector containing LdPDEA, P2 = 5.9 ± 0.5%; (f) cells bearing vector with LdPDEA and exposed to H_2O_2, P2 = 33.3 ± 3.0%; (g) cells bearing vector with LdPDEA and preincubated under differentiation conditions, P2 = 8.4 ± 0.7%; (h) cells bearing vector with LdPDEA, preincubated under differentiation conditions, and exposed to H_2O_2, P2 = 28.5 ± 2.7%. (D) Activated macrophages (pretreated with 500 U/ml IFN-γ for 24 h) were infected with *L. donovani* promastigotes bearing either empty vector or vector containing LdPDEA and preexposed to differentiation conditions for various times between 0 and 12 h. The numbers of intracellular amastigotes were determined by propidium iodide staining. Values are means ± SD ($n = 3$). $^{**}p<0.01$ vs control.

peroxidases, which in turn, might shift the bias of TSH utilization toward antioxidant defense.

Effects of PDEA overexpression on parasite resistance against pro-oxidants

To further ascertain the functional significance of PDEA, a strain of *L. donovani* promastigotes bearing the PDEA gene in the pTEX plasmid (a trypanosome-specific shuttle vector, a kind gift from Dr. Martin Taylor, London School of Hygiene and Tropical Medicine, London, UK) was generated. A 3- to 3.5-fold increase in LdPDEA together with a marked decrease in intracellular cAMP levels was observed in overexpressing cells compared to wild type as reported earlier [13]. On exposure to differentiation conditions (37°C and pH 5.5), control cells (bearing an empty pTEX vector) exhibited substantially decreased PDEA levels (~2.1-, ~2.2-, and ~3.2-fold after 3, 6, and 12 h exposure, respectively, Fig. 8A). On the other hand, in PDEA-overexpressing cells, PDEA remained almost unaltered up to 6 h of exposure to differentiation conditions and the level was reduced by only ~1.5-fold after 12 h exposure (Fig. 8B). We then wanted to determine the peroxide neutralization capacity of the overexpressing cells by FACS analysis using H_2DCFDA. Cells, either exposed or unexposed to differentiation conditions (37°C and pH 5.5), were subjected to FACS analysis and a gate (P2) was established that delineated the upper 5% of fluorescent cells. In the case of PDEA-overexpressing cells, the percentage of cells in the P2 gate did not differ significantly when exposed to differentiation conditions (27.4 ± 2.5 vs 20.1 ± 2.0, $n = 4$, $p < 0.01$), whereas in the case of cells bearing empty vector, the percentage of cells in the P2 gate was reduced significantly (32.0 ± 3.0 vs 12.0 ± 1.4, $n = 4$, $p < 0.01$), suggesting thereby that these cells are more efficient in peroxide neutralization when exposed to differentiation conditions than the PDEA-overexpressing cells under similar conditions (Fig. 8C). Differentiation condition-induced resistance against oxidative damage in these cells was further determined by assessing the infectivity of the parasites toward IFN-γ-activated macrophages. As shown in Fig. 8D, promastigotes overexpressing PDEA were 1.6 ± 0.1- and 1.5 ± 0.1-fold less infective toward IFN-γ-activated macrophages after exposure to differentiation conditions for 6 and 12 h, respectively ($n = 3$), compared to promastigotes bearing empty vector as assessed by intramacrophage survival. Taken together, these results suggest that differentiation conditions might have triggered depletion of PDEA, which, in turn, might be involved in inducing resistance against oxidative damage.

Discussion

Mining of the *Leishmania* genome revealed the presence of genes associated with the cAMP signaling pathway, and our previous work showed that differentiation conditions can induce resistance to oxidative damage via a cAMP-mediated response in *L. donovani* [13]. However, a defined participation of any of those genes in environmental sensing as well as in differentiation-coupled events is yet to be determined. The results of this study show that differentiation-coupled depletion of a cytosolic cAMP PDE may be a prerequisite for promastigotes to be able to detoxify ROS and RNI encountered during invasion of activated macrophages. Modulation of PDEs is important in regulating the trypanothione biosynthetic pathway as well as the trypanothione pool utilization of the parasite, which, in turn, affects the ROS and RNI neutralization capacity.

Although cAMP signaling is known to be spatiotemporally located in eukaryotes, definite compartmentalized cAMP signaling is yet to be reported in kinetoplastidae. However, subcellular localization of cAMP modulating enzymes in *Trypanosoma* indicates the presence of a cAMP response regulation there [17–19]. The genome sequences of *Trypanosoma* and *Leishmania* spp. suggest that these parasites encode soluble PDEs and adenylate cyclases, indicating a cytosolic cAMP regulatory machinery in these parasites (http://www.ebi.ac.uk/parasites/leish.html). In *Dictyostelium discoideum,* several cytosolic PDEs regulate the intracellular cyclic nucleotide pool, affecting differentiation of the organism [35]. In this study, a significantly reduced PDE activity in the cytosolic fraction of amastigotes with an almost unaltered level in the membrane fraction suggests a regulatory relationship of cytosolic PDEs with differentiation conditions in *L. donovani.* In contrast to mammalian class I PDEs, LdPDEA showed a higher K_M for cAMP (166.66 μM). The high K_M might reflect an artifact due to bacterial expression, but this seems unlikely as mammalian class I PDEs have been expressed in similar strains of *E. coli* and were shown to exhibit the characteristic specificities and low K_M values for their respective substrates [36–38]. Moreover, LdPDEA, when expressed in HEK293 cells, exhibited similar K_M values (data not shown). Cyclic nucleotide PDEs have been found to play a significant role in regulating unicellular differentiation in *D. discoideum* and *Plasmodium falciparum,* in which stage-specific expression of a cAMP-specific PDE (DdPDEE) and a cGMP-specific PDE (PfPDE1) has been documented [39,40]. Analysis of the expression of LdPDEA in various life-cycle stages revealed that the expression was markedly reduced during transformation of promastigotes to amastigotes, suggesting a possible role for PDEA in the differentiation of the parasite.

To study the role of PDEA in *L. donovani,* we used inhibitors such as etazolate and trequinsin. Because these inhibitors are not LdPDEA-specific and might affect the activities of other PDEs [22], a tetracycline-inducible PDEA knockdown system was constructed. The gene-silencing strategies work differentially in different kinetoplastid parasites, as a typical RNAi-mediated gene-silencing approach has been effectively used for *Trypanosoma,* but *Leishmania* seems to lack RNAi activity. However, antisense RNA-mediated gene silencing has been reported in knocking down gp63 and the superoxide dismutase gene in *L. amazonensis* and *L. tropica,* respectively [41,42]. Recently, tetracycline-induced gene silencing has been successfully applied to delineate a functional tRNA import complex in *L. tropica* [43] and to identify minimal functionally interacting fragments of topoisomerase 1B using *L. tarentolae* [44]. Differentiation-associated depletion of PDEA suggests that PDEA might have a role in prolonging cAMP elevation in the soluble fraction and this effect may be important for the induction of resistance against toxic oxidants, as PDEA depletion indeed enhanced the ability to neutralize peroxide. Interestingly, PDEA-silenced cells showed relatively less peroxide resistance in comparison to inhibitor-treated cells. This might be due to a lower elevation of total intracellular cAMP in these cells compared to the inhibitor-treated cells, in which low K_M PDEB1 and B2 were also likely to be inhibited, resulting in greater elevation of cAMP levels.

Although the availability of TSH biosynthesis precursors such as arginine and putrescine was not affected by PDE inhibition, arginase and ODC expression, as well as activity, was increased in PDE inhibitor-treated cells or PDEA-silenced cells. Despite the elevation of arginase and ODC activity, no significant alteration in total thiol or TSH levels was detectable, suggesting that elevated arginase and ODC activity might have other implications in altering endogenous polyamine levels, which have been reported to be associated with differentiation of unicellular eukaryotes such as *D. discoideum* and *P. falciparum* [45,46]. Regulation of the TSH pool is necessary, as the parasite encounters distinct environmental changes in the course of its infective cycle. Analysis of the expression of trypanothione peroxidase and ascorbate peroxidase in PDEA-inhibited cells revealed upregulation of these enzymes, indicating a possible shift in the TSH pool utilization bias toward antioxidative defense. Such observation is interesting, as in the course of infection, after exposure to 37°C and pH 5.5, the parasite undergoes a block in cell-cycle progression at the G1 stage for around 8 h [47], which should reduce deoxyribonucleotide generation for which TSH is necessary. In such a situation an elevation

of TSH-utilizing antioxidants might be a preadaptation for resisting upcoming pro-oxidant exposure during macrophage invasion.

As a consequence of its unusual gene expression machinery, with transcription of polycistronic mRNA and maturation of individual genes by coordinated transplicing and polyadenylation, *Leishmania* gene expression does not seem to be regulated at the level of transcription, and therefore expression of genes located at different loci seems unlikely to be regulated by a single effector such as cAMP. However, stage-specific expression of a number of genes has been shown to be regulated via mRNA stability [48] and this, in turn, causes an ordered progression of transient and permanent up- or down-regulation of several hundred genes during differentiation [49,50]. In a number of mammalian cell lines, cAMP has been found to enhance the activity of specific enzymes such as phosphoenolpyruvate carboxykinase, lipoprotein lipase, steroidogenic acute regulatory protein, rennin, and sodium glucose cotransporter via enhanced mRNA stability [51–53]. Because in *Leishmania* the regulation of cell-cycle-specific gene expression has recently been reported [54], a cell-cycle-specific global regulatory event might be associated with the upregulation of the antioxidant genes. In this study, we demonstrate that depletion of PDEA might contribute to a sustained cAMP response in the cytosol of the parasite, and this sustained response might be one of the regulators of a differentiation-coupled shift in TSH utilization bias. Although, for a high K_M PDE, regulation of a phenotype such as a stress response seems unlikely, the observation is reminiscent of PDE1 from *Saccharomyces cerevisiae*, a high K_M class II PDE, which has been reported to play a major role in the quenching of short-term cAMP peaks upon metabolic stimulation without conferring any specific phenotype [55]. Moreover, a high K_M PDE from *D. discoideum* (PDE6) is known to play a significant role in regulating the cytosolic cAMP pool [35], and the *S. cerevisiae* PDE1 homologue in *Cryptococcus neoformans* regulates the intracellular cAMP pool as well as virulent attributes [56]. Although the impact of LdPDEA in regulating the basal level of cAMP seems not to be very significant in terms of affinity toward cAMP, it might regulate the cytosolic cAMP pool, which is important for regulation of global events such as mRNA stability and regulation of enzyme activity. This study suggests the significance of a cytosolic high K_M PDE in regulating differentiation-associated events that ultimately affect the infectivity of *L. donovani*. Moreover, this is the first time any physiological significance could be attributed to a high K_M class I PDE in this parasite.

Acknowledgments

This work was funded by the Department of Science and Technology and a Network Project grant (NWP 0038) from the Council of Scientific and Industrial Research (Government of India).

Appendix A. Supplementary data

Supplementary data associated with this article can be found, in the online version, at doi:10.1016/j.freeradbiomed.2009.08.025.

References

[1] Krauth-Seigel, L. R.; Comini, M. A.; Schlecker, T. The trypanothione system. *Subcell. Biochem.* **44:**231–251; 2007.
[2] Krauth-Siegel, R. L.; Meiering, S. K.; Schmidt, H. The parasite-specific trypanothione metabolism of *Trypanosoma* and *Leishmania*. *Biol. Chem.* **384:**539–549; 2003.
[3] Roberts, S. C.; Jiang, Y.; Jardim, A.; Carter, N. S.; Heby, O.; Ullman, B. Genetic analysis of spermidine synthase from *Leishmania donovani*. *Mol. Biochem. Parasitol.* **115:**217–226; 2001.
[4] Shaked-Mishan, P.; Suter-Grotemeyer, M.; Yoel-Almagor, T.; Holland, N.; Zilberstein, D.; Rentsch, D. A novel high-affinity arginine transporter from the human parasitic protozoan *Leishmania donovani*. *Mol. Microbiol.* **60:**30–38; 2006.
[5] Hasne, M. P.; Ullman, B. Identification and characterization of a polyamine permease from the protozoan parasite *Leishmania major*. *J. Biol. Chem.* **280:** 15188–15194; 2005.
[6] Dormeyer, M.; Reckenfelderbaumer, N.; Ludemann, H.; Krauth-Siegel, R. L. Trypanothione-dependent synthesis of deoxyribonucleotides by *Trypanosoma brucei* ribonucleotide reductase. *J. Biol. Chem.* **276:**10602–10606; 2001.
[7] Mukhopadhyay, R.; Dey, S.; Xu, W.; Gage, D.; Lightbody, J.; Ouellette, M.; Rosen, B. P. Trypanothione overproduction and resistance to antimonials and arsenicals in *Leishmania*. *Proc. Natl. Acad. Sci. USA* **93:**10383–10387; 1996.
[8] Alvarez-Curto, E.; Saran, S.; Meima, M.; Zobel, J.; Scott, C.; Schaap, P. cAMP production by adenylyl cyclase G induces prespore differentiation in *Dictyostelium* slugs. *Development* **134:**959–966; 2007.
[9] Ono, T.; Cabrita-Santos, L.; Leitao, R.; Bettiol, E.; Purcell, L. A.; Diaz-Pulido, O.; Andrews, L. B.; Tadakuma, T.; Bhanot, P.; Mota, M. M.; Rodriguez, A. Adenylyl cyclase alpha and cAMP signaling mediate *Plasmodium* sporozoite apical regulated exocytosis and hepatocyte infection. *PLoS Pathog.* **e1000008:**4; 2008.
[10] Abel, E. S.; Davids, B. J.; Robles, L. D.; Loflin, C. E.; Gillin, F. D.; Chakrabarti, R. Possible roles of protein kinase A in cell motility and excystation of the early diverging eukaryote *Giardia lamblia*. *J. Biol. Chem.* **276:**10320–10329; 2001.
[11] Vassella, E.; Reuner, B.; Yutzy, B.; Boshart, M. Differentiation of African trypanosomes is controlled by a density sensing mechanism which signals cell cycle arrest via the cAMP pathway. *J. Cell Sci.* **110:**2661–2671; 1997.
[12] Genestra, M.; Cysne-Finkelsteil, L.; Leon, L. Protein kinase A activity is associated with metacyclogenesis in *Leishmania amazonensis*. *Cell Biochem. Funct.* **22:** 315–320; 2004.
[13] Bhattacharya, A.; Biswas, A.; Das, P. K. Role of intracellular cAMP in differentiation-coupled induction of resistance against oxidative damage in *Leishmania donovani*. *Free Radic. Biol. Med.* **44:**779–794; 2008.
[14] Sanchez, M. A.; Zeoli, D.; Klamo, E. M.; Kavanaugh, M. P.; Landfear, S. M. A family of putative receptor-adenylate cyclases from *Leishmania donovani*. *J. Biol. Chem.* **270:** 17551–17558; 1995.
[15] Bieger, B.; Esser, L. O. Crystallization and preliminary X-ray analysis of the catalytic domain of the adenylate cyclase GRESAG4.1 from *Trypanosoma brucei*. *Acta Crystallogr. D Biol. Crystallogr.* **56:**359–362; 2000.
[16] Naula, C.; Schaub, R.; Leech, V.; Melville, S.; Seebeck, T. Spontaneous dimerization and leucine-zipper induced activation of the recombinant catalytic domain of a new adenylyl cyclase of *Trypanosoma brucei*, GRESAG4.4B. *Mol. Biochem. Parasitol.* **112:**19–28; 2001.
[17] Nolan, D. P.; Rolin, S.; Rodriguez, J. R.; Van Den Abbeele, J.; Pays, E. Slender and stumpy bloodstream forms of *Trypanosoma brucei* display a differential response to extracellular acidic and proteolytic stress. *Eur. J. Biochem.* **267:** 18–27; 2000.
[18] Oberholzer, M.; Marti, G.; Baresic, M.; Kunz, S.; Helphill, A.; Seebeck, T. The *Trypanosoma brucei* cAMP phosphodiesterases TbrPDEB1 and TbrPDEB2: flagellar enzymes that are essential for parasite virulence. *FASEB J.* **21:**720–731; 2007.
[19] Alonso, G. D.; Schoijet, A. C.; Torres, H. N.; Flawia, M. M. TcPDE4, a novel membrane-associated cAMP-specific phosphodiesterase from *Trypanosoma cruzi*. *Mol. Biochem. Parasitol.* **145:**40–49; 2006.
[20] Kunz, S.; Kloeckner, T.; Essen, L. O.; Seebeck, T.; Boshart, M. TbPDE1, a novel class I phosphodiesterase of *Trypanosoma brucei*. *Eur. J. Biochem.* **271:**637–647; 2004.
[21] Alonso, G. D.; Schoijet, A. C.; Torres, H. N.; Flawia, M. M. TcrPDEA1, a cAMP-specific phosphodiesterase with atypical pharmacological properties from *Trypanosoma cruzi*. *Mol. Biochem. Parasitol.* **152:**72–79; 2007.
[22] Johner, A.; Kunz, S.; Linder, M.; Shakur, Y.; Seebeck, T. Cyclic nucleotide specific phosphodiesterases of *Leishmania major*. *BMC Microbiol.* **6:**25; 2006.
[23] Wang, H.; Yan, Z.; Geng, J.; Kunz, S.; Seebeck, T.; Ke, H. Crystal structure of the *Leishmania major* phosphodiesterase LmjPDEB1 and insight into the design of the parasite-selective inhibitors. *Mol. Microbiol.* **66:**1029–1038; 2007.
[24] Miller, M. A.; McGowan, S. E.; Gantt, K. R.; Champion, M.; Novick, S. L.; Andersen, K. A.; Bacchi, C. J.; Yarlett, N.; Britigan, B. E.; Wilson, M. E. Inducible resistance to oxidant stress in the protozoan *Leishmania chagasi*. *J. Biol. Chem.* **275:** 33883–33889; 2000.
[25] Schilling, R. J.; Morgan, D. R.; Kilpatrick, B. F. A high-throughput assay for cyclic nucleotide phosphodiesterases. *Anal. Biochem.* **216:**154–158; 1994.
[26] Carter, W. O.; Narayanan, P. K.; Robinson, J. P. Intracellular hydrogen peroxide and superoxide anion detection in endothelial cells. *J. Leukocyte Biol.* **55:**253–258; 1994.
[27] Corraliza, I. M.; Campo, M. L.; Soler, G.; Modolell, M. Determination of arginase activity in macrophages: a micromethod. *J. Immunol. Methods* **174:**231–235; 1994.
[28] Hanson, S.; Adelman, J.; Ullman, B. Amplification and molecular cloning of the ornithine decarboxylase gene of Leishmania donovani. *J. Biol. Chem.* **267:** 2350–2359; 1992.
[29] Kandpal, M.; Fouce, R. B.; Pal, A.; Guru, P. Y.; Tekwani, B. L. Kinetics and molecular characteristics of arginine transport by *Leishmania donovani* promastigotes. *Mol. Biochem. Parasitol.* **71:**193–201; 1995.
[30] Kelly, J. M.; Ward, H. M.; Miles, M. A.; Kendall, G. A shuttle vector which facilitates the expression of transfected genes in *Trypanosoma cruzi* and *Leishmania*. *Nucleic Acids Res.* **20:**3963–3969; 1992.
[31] Das, A.; Dasgupta, A.; Sharma, S.; Ghosh, M.; Sengupta, T.; Bandopadhyay, S.; Majumder, H. K. Characterisation of the gene encoding type II DNA topoisomerase from *Leishmania donovani:* a key molecular target in antileishmanial therapy. *Nucleic Acids Res.* **29:**1844–1851; 2001.
[32] Gaur, U.; Roberts, S. C.; Dalvi, R. P.; Corraliza, I.; Ullman, B.; Wilson, M. E. An effect of parasite-encoded arginase on the outcome of murine cutaneous leishmaniasis. *J. Immunol.* **179:**8446–8453; 2007.

[33] Iniesta, V.; Gomez-Nieto, L. C.; Corraliza, I. The inhibition of arginase by N(omega)-hydroxy-L-arginine controls the growth of *Leishmania* inside macrophages. *J. Exp. Med.* **193:**777–784; 2001.
[34] Coons, T.; Hanson, S.; Bitoni, A. J.; McCann, P. P.; Ullman, B. Alpha-difluoromethylornithine resistance in *Leishmania donovani* is associated with increased ornithine decarboxylase activity. *Mol. Biochem. Parasitol.* **39:**77–89; 1990.
[35] Bader, S.; Kortholt, A.; Van Haastert, P. J. Seven *Dictyostelium discoideum* phosphodiesterases degrade three pools of cAMP and cGMP. *Biochem. J.* **402:** 153–161; 2007.
[36] Sung, B. J.; Yeon Hwang, K.; Ho Jeon, Y.; Lee, J. I.; Heo, Y. S.; Hwan Kim, J.; Moon, J.; Min Yoon, J.; Hyun, Y. L.; Kim, E.; Jin Eum, S.; Park, S. Y.; Lee, J. O.; Gyu Lee, T.; Ro, S.; Myung Cho, J. Structure of the catalytic domain of human phosphodiesterase 5 with bound drug molecules. *Nature* **425:**98–102; 2003.
[37] Huai, Q.; Wang, H.; Sun, Y.; Kim, H. Y.; Liu, Y.; Ke, H. Three-dimensional structures of PDE4D in complex with rolipram and implication on inhibitor selectivity. *Structure (Cambridge)* **11:**865–873; 2003.
[38] Sullivan, M.; Egerton, M.; Shakur, Y.; Marquardsen, A.; Houslay, M. D. Molecular cloning and expression, in both COS-1 cells and *S. cerevisiae,* of a human cytosolic type-IVA, cyclic AMP specific phosphodiesterase (hPDE-IVA-h6.1). *Cell Signalling* **6:**793–812; 1994.
[39] Meima, M. E.; Weening, K. E.; Schaap, P. Characterization of a cAMP-stimulated cAMP phosphodiesterase in *Dictyostelium discoideum*. *J. Biol. Chem.* **278:** 14356–14362; 2003.
[40] Taylor, C. J.; McRobert, L.; Baker, D. A. Disruption of a Plasmodium falciparum cyclic nucleotide phosphodiesterase gene causes aberrant gametogenesis. *Mol. Microbiol.* **69:**110–118; 2008.
[41] Chen, D. Q.; Kolli, B. K.; Yadava, N.; Lu, H. G.; Gilman-Sachs, A.; Peterson, D. A.; Chang, K. P. Episomal expression of specific sense and antisense mRNAs in *Leishmania amazonensis:* modulation of gp63 level in promastigotes and their infection of macrophages in vitro. *Infect. Immun.* **68:**80–86; 2000.
[42] Ghosh, S.; Goswami, S.; Adhya, S. Role of superoxide dismutase in survival of *Leishmania* within the macrophage. *Biochem. J.* **369:**447–452; 2003.
[43] Goswami, S.; Dhar, G.; Mukherjee, S.; Mahata, B.; Chatterjee, S.; Home, P.; Adhya, S. A bifunctional tRNA import receptor from *Leishmania* mitochondria. *Proc. Natl. Acad. Sci. USA* **103:**8354–8359; 2006.
[44] Bosedasgupta, S.; Das, B. B.; Sengupta, S.; Ganguly, A.; Roy, A.; Tripathi, G.; Majumder, H. K. Amino acids 39–456 of the large subunit and 210–262 of the small subunit constitute the minimal functionally interacting fragments of the unusual heterodimeric topoisomerase IB of *Leishmania*. *Biochem. J.* **409:**481–489; 2008.
[45] Saran, S. Changes in endogenous polyamine levels are associated with differentiation in *Dictyostelium discoideum*. *Cell Biol. Int.* **22:**575–580; 1998.
[46] Muller, S.; Da'dara, A.; Luersen, K.; Wrenger, C.; Das Gupta, R.; Madhubala, R.; Walter, R. D. In the human malaria parasite *Plasmodium falciparum,* polyamines are synthesized by a bifunctional ornithine decarboxylase, S-adenosylmethionine decarboxylase. *J. Biol. Chem.* **275:**8097–8102; 2000.
[47] Saar, Y.; Ransford, A.; Waldman, E.; Mazareb, S.; Amin-Spector, S.; Plumblee, J.; Turco, S. J.; Zilberstein, D. Characterization of developmentally-regulated activities in axenic amastigotes of *Leishmania donovani*. *Mol. Biochem. Parasitol.* **95:**9–20; 1998.
[48] Wu, Y.; El Fakhry, Y.; Sereno, D.; Tamar, S.; Papadopoulou, B. A new developmentally regulated gene family in *Leishmania* amastigotes encoding a homolog of amastin surface proteins. *Mol. Biochem. Parasitol.* **110:**345–357; 2000.
[49] Saxena, A.; Lahav, T.; Holland, N.; Aggarwal, G.; Anupama, A.; Huang, Y.; Volpin, H.; Myler, P. J.; Zilberstein, D. Analysis of the *Leishmania donovani* transcriptome reveals an ordered progression of transient and permanent changes in gene expression during differentiation. *Mol. Biochem. Parasitol.* **152:**53–65; 2007.
[50] Saxena, A.; Worthey, E. A.; Yan, S.; Leland, A.; Stuart, K. D.; Myler, P. Evaluation of differential gene expression in *Leishmania major* Friedlin procyclics and metacyclics using DNA microarray analysis. *Mol. Biochem. Parasitol.* **129:**103–114; 2003.
[51] Wu, W.; Silbajoris, R. A.; Cao, D.; Bromberg, P. A.; Zhang, Q.; Peden, D. B.; Samet, J. M. Regulation of cyclooxygenase-2 expression by cAMP response element and mRNA stability in a human airway epithelial cell line exposed to zinc. *Toxicol. Appl. Pharmacol.* **231:**260–266; 2008.
[52] Duan, H.; Jefooate, C. R. The predominant cAMP-stimulated 3×5 kb StAR mRNA contains specific sequence elements in the extended 3′UTR that confer high basal instability. *J. Mol. Endocrinol.* **38:**159–179; 2007.
[53] Morris, B. J.; Adams, D. J.; Beveridge, D. J.; van der Weyden, L.; Mangs, H.; Leedman, P. J. cAMP controls human renin mRNA stability via specific RNA-binding proteins. *Acta Physiol. Scand.* **181:**369–373; 2004.
[54] Zick, A.; Onn, I.; Bezalel, R.; Margalit, H.; Shlomai, J. Assigning functions to genes: identification of S-phase expressed genes in *Leishmania major* based on post-transcriptional control elements. *Nucleic Acids Res.* **33:**4235–4242; 2005.
[55] Ma, P.; Wera, S.; Van Dijck, P.; Thevelein, J. M. The PDE1-encoded low-affinity phosphodiesterase in the yeast *Saccharomyces cerevisiae* has a specific function in controlling agonist-induced cAMP signaling. *Mol. Biol. Cell* **10:**91–104; 1999.
[56] Hicks, J. K.; Bahn, Y. S.; Heitman, J. Pde1 phosphodiesterase modulates cyclic AMP levels through a protein kinase A-mediated negative feedback loop in *Cryptococcus neoformans*. *Eukaryotic Cell* **4:**1971–1981; 2005.